JOURNAL OF CATALYSIS 111, 264–272 (1988)

Kinetics of Photocatalytic Oxidation of Organic Solutes over Titanium Dioxide

RALPH W. MATTHEWS

CSIRO Division of Energy Chemistry, Lucas Heights Research Laboratories, Private Mail Bag 7, Menai, New South Wales 2234, Australia

Received May 12, 1987; revised January 4, 1988

The kinetics of photooxidation to CO_2 of 22 organic solutes over a UV illuminated film of Degussa P25 titanium dioxide have been studied over a 100-fold concentration range for each solute, generally from about 1 to 100 mg liter^{-1}. The dependence of the photooxidation rate on concentration obeyed a simple two-coefficient Langmuir expression for each solute. The coefficients reflecting the degree of adsorption on the TiO_2 and the limiting rate at high concentrations enable the prediction of photocatalytic rates in any TiO_2-based photoreactor of a similar type once a reference rate has been determined for one of the solutes. A reaction mechanism is proposed for the oxidation of aromatic compounds involving peroxyhydroxycyclohexadienyl- and mucondialdehyde-type compounds as important intermediates. The solutes studied were benzoic acid, salicylic acid, phenol, biphthalate, 2-chlorophenol, 4-chlorophenol, monochlorobenzene, nitrobenzene, methanol, ethanol, *n*-propanol, 2-propanol, acetone, ethyl acetate, acetic acid, formic acid, sucrose, 2-naphthol, umbelliferone, chloroform, trichloroethylene, and dichloroethane.

INTRODUCTION

The photocatalytic oxidation of organic compounds in aqueous suspensions of titanium dioxide is a comparatively new method for the removal of impurities from water. It has possible application in the treatment of both waste waters and drinking water. Many compounds have been shown to be oxidized to carbon dioxide by this method (*1–20*). The photoactivating light required is near UV (<400 nm) or sunlight. The method has been found to be generally applicable to the destruction of trihalomethanes in water (*4–6, 8–10, 14*).

Usually the titanium dioxide has been present as a powder suspension and the destruction of compounds has been studied using closed systems. Recently, it was reported that titanium dioxide could be readily attached to glass surfaces allowing the TiO_2 to be illuminated as a stationary phase with water passing over the catalyst (*21, 22*). Thus open system continuous operation is possible.

It is noted that where the concentration dependence has been studied, the destruction of compounds over illuminated TiO_2 always follows a Langmuir adsorption isotherm. That is, the rate of destruction is not directly proportional to concentration and meaningful comparisons of rates of destruction between different compounds cannot be made at single concentrations. Thus a strongly adsorbed solute may undergo destruction at a significant rate at parts per million concentrations (*23*) even though it may be comparatively resistant to oxidation at high concentrations. The estimation of the destruction rate at any particular concentration requires a knowledge of the Langmuir–Hinshelwood kinetics for the compound.

In this work the oxidation to carbon dioxide of 22 common organic contaminants in water has been studied over a range of concentrations under identical photocatalytic oxidation conditions. As for other compounds, the rates of destruction fitted Langmuir–Hinshelwood kinetics and the

0021-9517/88 $3.00

parameters were determined for each compound. Thus the destruction rate of a compound relative to another compound may be estimated at any particular concentration.

EXPERIMENTAL

Materials

All chemicals were at least laboratory reagent grade and were obtained from reputable suppliers. Stock solutions were prepared using water from a Millipore Waters Milli Q water purification system. The titanium dioxide photocatalyst was Degussa P25 grade, surface area 50 ± 15 $m^2\ g^{-1}$, shown by X-ray diffraction analysis to be predominantly in the anatase form.

Apparatus

The TiO_2 photocatalyst (75 mg) was coated on the inside of a 7-m-long 65-turn spiral of borosilicate glass tubing with 6-mm o.d., a 1-mm wall thickness, and a spiral volume of 90 cm^3 as previously described (*22, 39*). A 32.5-mm-diameter NEC 20-W black light blue fluorescent tube fitted snugly down the center of the spiral and was mounted in a standard 20-W fluorescent tube domestic lamp holder. The solution (40 ml) of the given organic solute being studied was circulated through the spiral and around a loop by means of a Cole–Parmer Model 7554-00 peristaltic pump. Viton flexible tubing was used in the pump and for connections to the various components. The solution was added at a loading port. Air was pumped around the loop and became entrained in the liquid at a tee junction, the bubbles passing up the spiral in serried ranks and separating from the liquid at the loading port before passing through a conductivity cell and returning to the loop. Because of the rapid intermingling of the gas and liquid phases in the spiral, carbon dioxide equilibration between the phases was rapidly established and the conductivity of the water in the cell increased with carbon dioxide concentration. The conductivity was measured with an Alpha 800 conductivity meter. The apparatus was calibrated by additions of measured volumes of carbon dioxide under conditions identical to those used in the experiments.

Procedure

As the analysis for carbon dioxide relies on a distribution between gas and liquid phases and the total volume of the closed system was constant, the same volume of solution was used in each run. Different concentrations of the same solute were obtained by varying the volume of water initially present in the photooxidation spiral loop so that when the required volume of organic stock solution was added, the total volume became 40 ml. The water in the spiral was also acidified with perchloric acid so that after the addition of the organic solute, the pH was approximately 3.6. In a typical run, 39 ml of acidified water was circulated through the spiral with the light on and the loading port open until the equilibrium conductivity was obtained and the water temperature reached 40°C.

The lamp was then switched off, 1.0 ml of the organic solution added, the loading port closed, and the light switched on. Simultaneously the stop watch was started and the progress of the reaction recorded at 1-min intervals for 10 min. This procedure was followed at eight different concentrations for each compound. Periodically, a benzoic acid solution was used to test for changes in the photocatalytic performance of the spiral. No significant change in the photooxidation rate was observed at any stage.

Actinometry

Potassium ferrioxalate solution and the analytical method of Hatchard and Parker (*24*) were used to measure the photon flux in the spiral before it was coated with TiO_2. Since the maximum emission of the lamp occurred at approximately 350 nm the quantum yield for ferrous ion formation in the ferrioxalate solution was taken to be 1.28 (*25*).

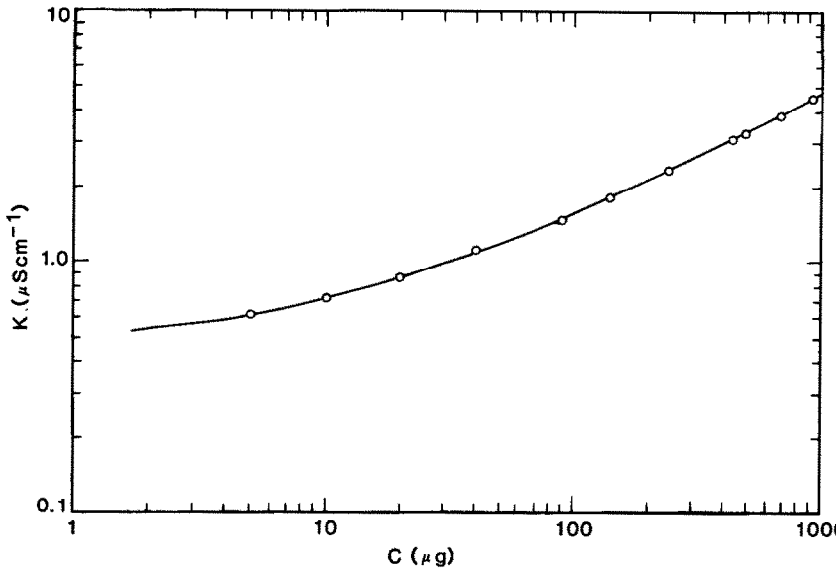

FIG. 1. Calibration curve using measured volumes of carbon dioxide. Conductivity versus weight of carbon in CO_2.

RESULTS

The addition of measured amounts of carbon dioxide to the apparatus gave the equilibrium specific conductance readings shown in Fig. 1. When the logarithm of the specific conductance expressed in microsiemens per centimeter was plotted against the logarithm of the amount of carbon expressed in micrograms, a smooth curve was obtained which became linear for amounts of carbon greater than 100 μg.

In the runs with various organic solutes added to the apparatus, the carbon oxidized to CO_2, indicated by the meter reading, was obtained from the calibration curve (Fig. 1) and plotted against the illumination time. A typical result for phenol is shown in Fig. 2. Although the plots were generally S shaped they were reasonably linear over 60–70% of the range of carbon oxidized with maximum linearity occurring closest to the 50% oxidation mark. The dashed lines in Fig. 2 were obtained by linear least-squares analysis of the experimental points lying within the range indicated by the dashed lines. From the slopes of these lines the oxidation rates expressed as milligrams of phenol per liter per minute were calculated and listed against the corresponding initial phenol concentration in Table 1. The other solutes were treated similarly. The oxidation rates for phenol are plotted against the initial phenol concentrations in Fig. 3 together with similar plots for some of the other solutes. As the plots for all the solutes were

TABLE 1

Oxidation Rates for Phenol Obtained by Least-Squares Analysis of Data in Fig. 2

Initial [phenol] (mg liter^{-1})	Oxidation rate	
	Experimental (mg liter^{-1} min^{-1})	Calculated (mg liter^{-1} min^{-1})
0.58	0.17 ± 0.02	0.14
1.46	0.44 ± 0.07	0.34
2.91	0.81 ± 0.04	0.66
5.83	1.46 ± 0.01	1.25
14.6	2.32 ± 0.07	2.63
29.1	4.24 ± 0.08	4.18
43.7	5.28 ± 0.09	5.20
58.3	5.88 ± 0.12	5.92

Note. Conditions: 20-W lamp, solution temp. 40°C, circulation at 300 ml min^{-1}.

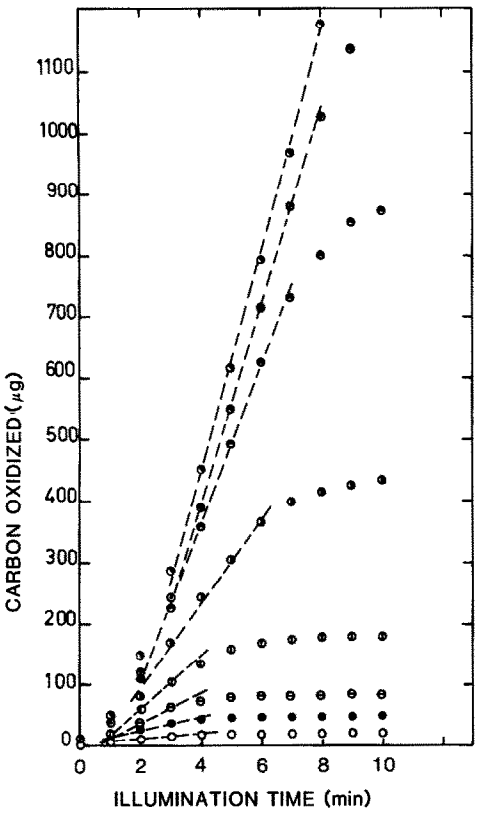

FIG. 2. Weight of carbon oxidized to CO_2 versus illumination time, 40 ml phenol solution each data set. lamp, 20 W; 300 ml min^{-1} circulation rate; 40°C; concentrations in milligrams per liter. (○) 0.58; (●) 1.46; (⊖) 2.91; (◫) 5.83; (◑) 14.6; (◓)29.1; (◎) 43.7; (◔) 58.3.

closely approximated by curves having the shape of Langmuir adsorption isotherms, the data sets for each solute were treated by the method of least squares assuming that the data were described by the expression

$$R = \frac{Kk_1[S]^0}{1 + k_1[S]^0}, \qquad (1)$$

where R is the rate of oxidation of the solute to CO_2, K, k_1 are proportionality constants for the solute, and $[S]^0$ is the initial concentration of the solute. In the case of phenol, the numerical parameters obtained by this analysis were 0.024 ± 0.004 mg^{-1} liter and 10.2 ± 0.9 mg $liter^{-1}$ min^{-1} for k_1 and K, respectively, and the line drawn through the experimental points in Fig. 3 is that calculated by substitution of these parameters in expression (1). The oxidation rates listed in Table 1, column 3, were also calculated with these values. Similar treatments of the data from the other solutes gave the parameters listed in Table 2.

A ferrous ion formation rate of 833 μM min^{-1} was found when 500 ml of 0.006 M potassium ferrioxalate was circulated through the photoreactor without TiO_2. A concentration change of 8.14 mM min^{-1} was therefore calculated for 40 ml of solution in which the quantum yield for the process is 1.0.

DISCUSSION

Reaction Mechanism

Published reaction mechanisms for the oxidation of aromatic hydrocarbons over titanium dioxide suspended in aerated aque-

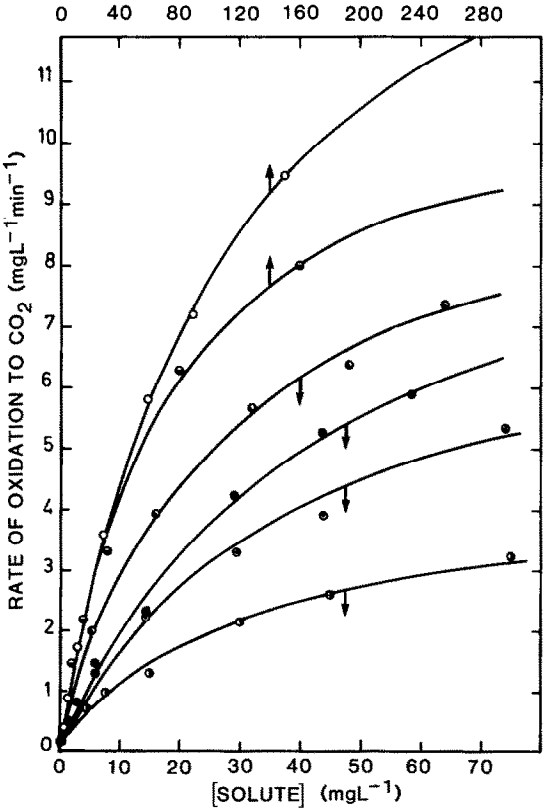

FIG. 3. Rates of oxidation to CO_2 versus initial solute concentrations. (◑) 2-Propanol; (◎) acetic acid; (●) phenol; (◔) 4-chlorophenol; (◒) methanol; (○) chloroform.

TABLE 2

Langmuir Parameters and Calculated Rates for Solutes at Different Concentrations

S	k_1 (mg^{-1} liter)	K (mg $liter^{-1}$ min^{-1})	Rate[a] (mg $liter^{-1}$ min^{-1})			
			1[b]	10[b]	50[b]	100[b]
Benzoic acid	0.0383 ± 0.007	8.1 ± 0.5	0.30	2.24	5.33	6.43
Salicyclic acid	0.036 ± 0.008	11.3 ± 1.1	0.39	2.99	7.26	8.84
Phenol	0.024 ± 0.004	10.2 ± 0.9	0.24	1.97	5.56	7.20
Biphthalate	0.023 ± 0.003	11.0 ± 0.7	0.24	2.06	5.88	7.67
2-Chlorophenol	0.010 ± 0.003	18.4 ± 4.1	0.18	1.67	6.13	9.20
4-Chlorophenol	0.038 ± 0.003	10.2 ± 0.3	0.37	2.81	6.68	8.10
Chlorobenzene	0.038 ± 0.007	6.4 ± 0.5	0.23	1.77	4.21	5.10
Nitrobenzene	0.062 ± 0.012	4.7 ± 0.3	0.27	1.79	3.55	4.00
Methanol	0.014 ± 0.002	11.5 ± 0.8	0.16	1.41	4.73	6.70
Ethanol	0.021 ± 0.003	10.1 ± 0.6	0.21	1.75	5.17	6.80
n-Propanol	0.020 ± 0.003	10.2 ± 0.6	0.20	1.70	5.10	6.80
2-Propanol	0.0350 ± 0.007	4.3 ± 0.4	0.14	1.11	2.74	3.34
Acetone	0.0165 ± 0.004	5.6 ± 0.6	0.09	0.79	2.53	3.50
Ethyl acetate	0.0158 ± 0.002	9.1 ± 0.6	0.14	1.24	4.02	5.60
Acetic acid	0.0265 ± 0.005	7.9 ± 0.5	0.20	1.65	4.50	5.70
Formic acid	0.0166 ± 0.003	21.4 ± 1.7	0.35	3.05	9.70	13.3
Sucrose	0.0270 ± 0.002	8.5 ± 0.3	0.22	1.81	4.88	6.20
2-Naphthol	0.044 ± 0.006	5.1 ± 0.4	0.21	1.55	3.48	4.10
Umbelliferone	0.0327 ± 0.006	6.5 ± 0.6	0.20	1.59	4.01	5.00
Chloroform	0.0090 ± 0.003	16.5 ± 0.2	0.15	1.36	5.12	7.80
Trichloroethylene	0.0091 ± 0.001	17.8 ± 0.8	0.16	1.48	5.56	8.50
Dichloroethane	0.0118 ± 0.002	7.9 ± 0.5	0.09	0.84	2.94	4.30

[a] Calculated from the expression $R = Kk_1[S]^0/(1 + k_1[S]^0)$.
[b] Initial concentration in milligrams per liter.

ous solutions involve ·OH radicals (*2, 26, 27*) produced by the reaction of photogenerated holes with adsorbed water or hydroxyl ions and also superoxide, $\cdot O_2^-$, or perhydroxyl, $HO_2\cdot$, radicals produced by reactions of the photoelectron with adsorbed oxygen (*2, 26–30*). More recently, Hashimoto *et al.* (*31*) have proposed that the direct oxidation of benzene of photogenerated holes also proceeds in competition with ·OH radical addition to the benzene ring, both reactions yielding the hydroxycyclohexadienyl radical (*32*). If this reaction is significant for benzene then it might also be significant for other aromatics. Okamoto *et al.* (*17*), however, consider that there is no significant direct oxidation pathway involving the photogenerated holes when phenol is the solute. Regardless of whether hydroxycyclohexadienyl radicals are formed via ·OH radical addition to the aromatic ring or via direct oxidation by the photogenerated holes, they react rapidly with oxygen to give peroxyhydroxycyclohexadienyl radicals leading to the simultaneous formation of phenol and the ring opened compound, mucondialdehyde (*33–37*). Similar reactions have been proposed by Getoff (*38*) for the radiation-induced decomposition of phenol in water. The mucondialdehyde is then further degraded to carbon dioxide and water. If the compound is a substituted aromatic, the mineral acid arising from the substituent will also be formed. These considerations lead to the following postulated reaction mechanism for the photooxidation of aromatics at the surface of TiO_2 catalyst,

$$TiO_2 \xrightarrow{h\nu} h^+ + e^- \quad (2)$$

$$h^+ + e^- \rightarrow \Delta \quad (3)$$

$$e^- + O_2 \rightarrow \cdot O_2^- \xrightarrow{H^+} HO_2\cdot \quad (4)$$

$$h^+ + 2H_2O \rightarrow \cdot OH + H_3O^+ \quad (5)$$

$$h^+ + OH^- \rightarrow \cdot OH \quad (6)$$

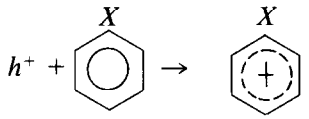

(7)

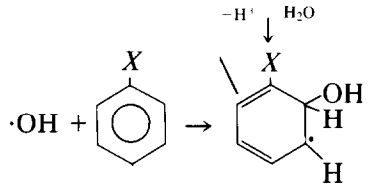

(8)

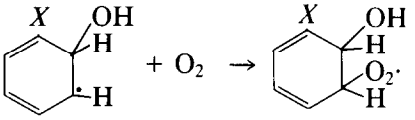

(9)

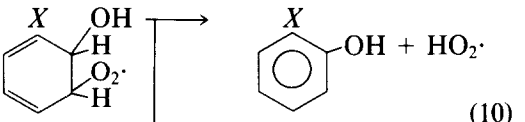

(10)

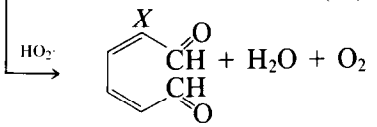

(11)

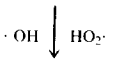

$$CO_2 + H_2O + HX \quad (12)$$

Reaction (10) leading to the corresponding phenol from the parent compound appears to be a minor reaction path (*39*), but this will also be eventually degraded to CO_2 since it will also be attacked by ·OH radicals or positive holes at the surface to form a series of reactions parallel to reactions (*7–12*).

Kinetics

It is postulated that both oxygen and the organic solutes are adsorbed at different sites on the surface of the TiO_2. It is known that ·OH radicals react rapidly with most organic solutes (*40*) and it seems likely that the positive holes would show similar reactivity. It is also known that oxygen reacts with the photoelectrons and should inhibit the electron–hole recombination reaction (*3*). The photodecomposition reaction of organic solutes should therefore be favored by high solute and oxygen concentrations. It is assumed that the rate-determining step is the reaction between the primary oxidizing species and the organic solute, S [reactions (7) and (8)]. In terms of Langmuir–Hinshelwood kinetics (*41*) the second-order decomposition rate at the surface forming CO_2 may be expressed as

$$R = k^1\theta_{O_2}\theta_S, \quad (13)$$

where θ_{O_2} and θ_S are the fractions of the sites covered by oxygen and the organic solute, respectively.

Because in this work the initial oxygen pressure was the ambient air-equilibrated value, θ_{O_2} may be regarded as constant and expression (13) can be rewritten as

$$R = k^{11}\theta_S. \quad (14)$$

The fraction of sites covered by organic solute, θ_S, can be expressed as (*42*)

$$\theta_S = \frac{k_1[S]}{1 + k_1[S] + \sum_i k_i[I_i]}, \quad (15)$$

where k_1 and k_i are equilibrium adsorption constants and S and I are the equilibrium solute and intermediate decomposition products. After the manner of Augugliaro *et al.* (*42*) the simplifying assumption is made that

$$k_1[S] + \sum_i k_i[I_i] = k_1[S]^0. \quad (16)$$

That is, it is assumed that the adsorption constants for the decomposition intermediates are the same as those for the original solute. This assumption is made solely as a simplifying step and without substantiation

from independent evidence. Substitution of expression (16) into (15) gives

$$\theta_S = \frac{k_1[S]}{1 + k_1[S]^0} \qquad (17)$$

and hence

$$R = k^{11} \frac{k_1[S]}{1 + k_1[S]^0}. \qquad (18)$$

The values of R were estimated at 50% decomposition, that is, when $[S] = 0.5[S]^0$. Therefore

$$R = K \frac{k_1[S]^0}{1 + k_1[S]^0}, \qquad (1)$$

where $K = 0.5k^{11}$. The data for the rates of oxidation to CO_2 of all solutes were well described by expression (1).

From the shape of the curves in Fig. 2 it is apparent that there is an induction period to the reaction. Since the equilibrium between the CO_2 released in the photoreactor and that absorbed in the conductivity cell was not instantaneously established, some apparent induction period was expected. However, if the time for equilibration was the only factor involved a constant induction period should have been observed. This was not the case; in general, the period increased with increasing solute concentration, suggesting that the intermediate decomposition products compete with the original solute for the photogenerated radical oxidizing species.

The data in Table 3 show a comparison between measured times for 50% decomposition of phenol solutions at different initial concentrations and times calculated in two different ways. In the first (column 3), the time was calculated by dividing 0.5 times the initial phenol concentration by the rate obtained from expression (1) and the k_1 and K values for phenol from Table 2. In the second (column 5), the integrated form of expression (1) was used (*39*),

$$t_{0.5} = \frac{0.5[S]^0}{K} + \frac{0.693}{k_1 K}. \qquad (19)$$

TABLE 3

Comparison between Experimental and Calculated Times for Conversion of 50% of Phenol to CO_2

Initial [phenol] (mg liter^{-1})	R (mg liter^{-1} min^{-1})	t^a calc. (min)	t exp. (min)	t^b calc. (min)
0.58	0.140	2.07	1.80	2.86
1.46	0.345	2.12	2.05	2.90
2.91	0.664	2.18	2.30	2.99
5.83	1.25	2.33	2.65	3.13
14.6	2.64	2.76	3.80	3.55
29.1	4.19	3.47	4.55	4.26
43.7	5.21	4.19	5.70	4.98
58.3	5.94	4.91	6.60	5.70

[a] Calculated using expression (1).
[b] Calculated using expression (19).

The increasing induction period at higher concentrations is reflected by the increasing deviation between experimental and calculated times as the concentration increases. Exceptions to this general behavior were formic acid and the chlorinated aliphatic hydrocarbons. These showed no evidence of significant increase in induction times with increasing concentration. This may be a consequence of a more direct conversion to CO_2 for these compounds than for the aromatics and other solutes.

Predicting Solute Oxidation Rates

The shapes of the rate of oxidation curves versus initial solute concentrations (Fig. 3) show a regime in which R is approximately proportional to $[S]$ when $k_1K[S]^0 \ll 1$ and a regime in which R is approximately equal to K when $k_1[S]^0 \gg 1$. The K values of Table 2 therefore represent the limiting oxidation rates for the solutes at high concentration. It is seen that the highest rate occurs with formic acid followed by 2-chlorophenol and trichloroethylene. The compounds most resistant to total oxidation were nitrobenzene and 2-propanol. The k_1 values reflect the tendency for the solutes to be adsorbed by the TiO_2, the higher values indicating a more rapid rate of oxidation at low concentrations. The highest

value for k_1 was obtained for nitrobenzene and the lowest for trichloroethylene and chloroform. Hence, although nitrobenzene was one of the most resistant to oxidation, its measured rate at low concentrations was not the lowest rate; the lowest rates at 1 mg liter^{-1} concentrations (column 4) were obtained for acetone and dichloroethane and the highest rate was for salicyclic acid.

Since the oxidation rates in Table 2 were calculated from data obtained under identical conditions, it should be possible to predict photooxidation rates over thin layers of Degussa P25 TiO_2 illuminated in any other experimental arrangement once a reference rate is established for one of the solutes listed.

Quantum Yield

The maximum rate of oxidation to CO_2 of the solutes listed in Table 2 was for formic acid. Under the experimental conditions (20-W lamp, 40°C, 300 ml min^{-1} circulation rate) the limiting rate was 21.4 mg liter^{-1} min^{-1} or 0.465 m*M* min^{-1}. Assuming that all the light is absorbed by the TiO_2 this corresponds to a quantum yield of 0.06 molecules of CO_2 per photon.

CONCLUSION

An apparatus has been built which facilitates the accumulation of data on the photocatalytic oxidation to carbon dioxide of organic solutes in aqueous solutions in contact with an illuminated layer of TiO_2. A reaction mechanism for the oxidation of aromatic compounds has been proposed and the reaction kinetics studied for each solute. Simplifying assumptions made are that intermediate decomposition products have the same adsorption equilibrium properties at the surface as the parent compound and that they are totally oxidized to CO_2. Reaction rates, estimated by regression analysis centered around data at 50% conversion of each solute, are well described by Langmuir–Hinshelwood kinetics. The Langmuir parameters for each solute, obtained under identical conditions, have been tabulated. The data provide a means of estimating photocatalytic oxidation rates to CO_2 for any of the 22 solutes at any concentration in other illuminated TiO_2 photoreactors of similar type once a reference rate for one of the compounds has been obtained.

REFERENCES

1. Bideau, M., Claudel, B., and Otterbein, M., *J. Photochem.* **14,** 291 (1980).
2. Izumi, I., Dunn, W. W., Wilbourn, K. O., Fan, F.-R. F., and Bard, A. J., *J. Phys. Chem.* **84,** 3207 (1980).
3. Herrmann, J.-M., Mozzanega, M.-N., and Pichat, P., *J. Photochem.* **22,** 333 (1983).
4. Hsiao, C.-Y., Lee, C.-L., and Ollis, D. F., *J. Catal.* **82,** 418 (1983).
5. Pruden, A. L., and Ollis, D. F., *J. Catal.* **82,** 404 (1983).
6. Pruden, A. L., and Ollis, D. F., *Environ. Sci. Technol.* **17,** 628 (1983).
7. Yoneyama, H., Takao, Y., Tamura, H., and Bard, A. J., *J. Phys. Chem.* **87,** 1417 (1983).
8. Ollis, D. F., Hsiao, C.-Y., Budiman, L., and Lee, C.-L., *J. Catal.* **88,** 89 (1984).
9. Ahmed, S., and Ollis, D. F., *Sol. Energy* **32,** 597 (1984).
10. Nguyen, T., and Ollis, D. F., *J. Phys. Chem.* **88,** 3386 (1984).
11. Kawaguchi, H., *Environ. Technol. Lett.* **5,** 471 (1984).
12. Barbeni, M., Pramauro, E., Pelizzetti, E., Borgarello, E., Gratzel, M., and Serpone, N., *Nouv. J. Chim.* **8,** 547 (1984).
13. Barbeni, M., Pramauro, E., Pelizzetti, E., Borgarello, E., and Serpone, N., *Chemosphere* **14,** 195 (1985).
14. Ollis, D. F., *Environ. Sci. Technol.* **19,** 480 (1985).
15. Hidaka, H., Kubota, H., Gratzel, M., Serpone, N., and Pelizzetti, E., *Nouv. J. Chim.* **9,** 67 (1985).
16. Pelizzetti, E., Barbeni, M., Pramauro, E., Serpone, N., Borgarello, E., Jamieson, M. A., and Hidaka, H., *Chim. Ind.* **67,** 623 (1985).
17. Okamoto, K.-J., Yamamoto, Y., Tanaka, H., Tanaka, M., and Itaya, A., *Bull. Chem. Soc. Japan* **58,** 2015 (1985).
18. Matthews, R. W., *Sunworld* **9,** 3 (1985).
19. Matthews, R. W., *J. Catal.* **97,** 565 (1986).
20. Matthews, R. W., *Water Res.* **20,** 569 (1986).
21. Serpone, N., Borgarello, E., Harris, R., Cahill, P., and Borgarello, M., *Sol. Energy Mater.* **14,** 121 (1986).
22. Matthews, R. W., *Sol. Energy* **38,** 405 (1987).
23. Brown, G. T., and Darwent, J. R., *J. Phys. Chem.* **88,** 4955 (1984).

24. Hatchard, C. G., and Parker, C. A., *Proc. R. Soc. London Ser. A* **235,** 518 (1956).
25. Demas, J. N., Bowman, W. D., Zalewski, E. F., and Velapoldi, R. A., *J. Phys. Chem.* **85,** 2766 (1981).
26. Fujihira, M., Satoh, Y., and Osa, T., *Nature (London)* **293,** 5829 (1981); *J. Electroanal. Chem. Interfacial Electrochem.* **126,** 277 (1981).
27. Matthews, R. W., *J. Chem. Soc. Faraday Trans. 1* **86,** 457 (1984).
28. Jaeger, C. D., and Bard, A. J., *J. Phys. Chem.* **83,** 3146 (1979).
29. Izumi, I., Fan, F.-R. F., and Bard, A. J., *J. Phys. Chem. 85,* 218 (1981).
30. Takagi, K., Fijioka, T., Sawaki, Y., and Iwamura, H., *Chem. Lett. Chem. Soc. Japan,* 913 (1985).
31. Hashimoto, K., Kawai, T., and Sakata, T., *J. Phys. Chem.* **88,** 4083 (1984).
32. Neta, P., and Fessenden, R. W., *J. Amer. Chem. Soc.* **99,** 163 (1977).
33. Loeff, I., and Stein, G., *J. Chem. Soc.,* 2623 (1963).
34. Dorfman, L. M., Taub, I. A., and Buhler, R. E., *J. Chem. Phys.* **36,** 3051 (1962).
35. Balakrishnan, I., and Reddy, M. P., *J. Phys. Chem.* **76,** 1273 (1972).
36. Irion, M. P., Fuss, W., and Kompa, K.-L., *Appl. Phys. B* **27,** 191 (1982).
37. Eberhardt, M. K., *J. Amer. Chem. Soc.* **103,** 3876 (1981).
38. Getoff, N., *Int. J. Appl. Radiat. Isot.* **37,** 1103 (1986).
39. Matthews, R. W., *J. Phys. Chem.* **91,** 3328 (1987).
40. Anbar, M., and Neta, P., *Int. J. Appl. Radiat. Isot.* **18,** 493 (1967).
41. Adamson, A. W., "Physical Chemistry of Surfaces," p. 544. Interscience, New York, 1960.
42. Augugliaro, U., Palmisano, L., Sclafari, A., Minero, C., and Pelizzetti, E., *Toxicol. Environ. Chem.,* in press.
43. Matthews, R. W., *Aust. J. Chem.* **40,** 667 (1987).